

# **EFFECT OF THE INITIAL GAS MALDISTRIBUTION ON THE PRESSURE DROP OF STRUCTURED PACKINGS**

**Z. Olujic, A. Mohamed Ali, P. J. Jansens**

Laboratory for Process Equipment, Delft University of Technology  
Delft, The Netherlands

## **ABSTRACT**

This paper presents results of a comprehensive, large scale experimental study devoted to establishing the relation between the quality of initial gas (mal)distribution, as created by common liquid collecting devices used in redistribution sections of packed columns, and the hydraulics of a structured packing bed. Both dry and wet bed experiments were conducted with air/water system under ambient conditions, using a 1.4 m ID Plexiglas column, including also high liquid loads. Additional, controlled gas maldistribution studies were conducted to observe the bed height needed to smooth out various types of initial maldistribution. From dry and wet experiments it appeared that the type (severity) of initial gas maldistribution influences the pressure drop of the bed.

*Key words: Distillation, packed columns, column internals, gas maldistribution, CFD*

## **INTRODUCTION**

Both experimental and modelling studies on liquid maldistribution and its effect on performance of structured packings have been widely published in the open literature. Controlled liquid maldistribution studies were performed on both small [1] and large-scale [2]. Recently, some effort was devoted to the characterisation of liquid maldistribution and establishing the relation between the quality of initial liquid distribution and the efficiency of a packed bed [3,4]. A most recent study by Billingham and Lockett [5] summarises the effort on modelling the effects of liquid maldistribution. Certainly, the quality of initial liquid distribution appeared to be critical and over the years distributor design practices were improved accordingly.

Comparatively, much less information is available on the relation between the performance of columns and the quality of initial gas or vapour maldistribution. Anyhow, certain research effort has been devoted to establishing and characterising the quality of initial gas distribution and some studies provided necessary design guidelines [6-12]. Most of the experimental work on pilot and particularly on large scale accompanied by

(3 m x 0.5 m x 4 m) structured packing bed [14] indicated that even a severe initial maldistribution could be smoothed out completely within a rather short bed height. Based on this observation it was suggested that the gas maldistribution, if present as such at all in the bulk of structured packing is negligible with respect to that of the liquid.

Edwards et al [4] developed a mathematical model capable of describing the depth of penetration of some typical forms of both gas and liquid initial maldistribution. Interesting here is that in their considerations the authors assume the same level of initial maldistribution for both phases, say  $\pm 25\%$ . In general, a value lower than 5% flow variation per irrigation point is considered as the high quality initial distribution and such performances are expected from the state of the art liquid distributors. In their consideration of the penetration depth, they considered five typical forms of initial maldistribution studied earlier by Zuiderweg et al. [18] and found a relationship between the form of initial gas maldistribution and the depth of penetration, using 3% as quality standard. Discussing the sensitivity of a packed bed to liquid maldistribution Billingham and Lockett [3] apply an equivalent approach for gas maldistribution. However based on general belief/experience that the gas maldistribution quickly corrects itself in a bed, less importance is attached to the sensitivity to gas- than to liquid maldistribution. Indeed, this really looks to be so, if we consider the results of a controlled maldistribution study carried out most recently with both random and structured packings at Fractionation Research Inc. [19]. Standard total reflux distillation tests indicated that the initial gas maldistribution has no effect at all on packing efficiency, which, regarding the nature of their experiments led to the conclusion that apparently a very short bed depth is sufficient to suppress even a severe form of the initial gas maldistribution.

This is in line with the results of above mentioned hydraulic study carried out with a large rectangular structured packing bed [14]. However, both the separated multi-inlet gas supply and rectangular column configuration used in this study are not quite representative for operation of a standard large diameter column. Practically all reported experimental efforts with larger size equipment are related to the quality of initial gas distribution as delivered by gas distributors installed in the bottom of the column. The work of Fan et al [10] gives an idea about the extent of initial maldistribution that can be expected, from different rather sophisticated commercial gas distributors employed in large diameter columns. The paper by Yuan and Li [11] is the only reference providing some quantitative information on the depth of penetration of initial gas maldistribution related to different types of gas inlet. They found that few layers of corrugated sheet structured packings of standard type and size are needed to smooth out initial maldistribution introduced by two standard gas inlets employed usually in columns of smaller diameter.

However, there is usually only one gas inlet per column, and a majority of operating packed columns contain several beds. This means that beds located in upper column sections receive initial gas profiles as delivered by devices used to collect the liquid leaving that particular bed. Authors are not aware of publications reporting on gas distribution performance of liquid collectors and associated hydraulic performance of structured packing beds.

In general, a liquid collector is designed to collect the liquid without much interference with the upcoming gas flow, to mix it and feed it, mostly through one or several downpipes to the liquid redistributor below. Although a liquid redistribution section consists often of a streamlined vane (chevron) type liquid collector placed above a narrow trough liquid distributor it still represents a major flow restriction for ascending gas flow and may cause severe gas maldistribution. Indeed as observed experimentally and visualised accordingly using a Computational Fluid Dynamics package [20-22], common liquid collectors stimulate clustering of high and low velocity zones with strikingly large velocity range. The observed huge differences in local velocities are much more pronounced than that established for the “Chinese hat” type of inlet gas distributor used in our studies [20, 21].

This becomes even of greater concern in conjunction with increasing trend in application of the so-called high capacity packings. Namely, with further reduction in already very low pressure drop of a structured packing there is practically no intrinsic means left in a packed bed to suppress imported (initial) gas maldistribution. With other words, the quality of inlet gas distribution becomes again a concern for packed column designers. Hence the design practices and means used for this purposes have to be re-evaluated and improved accordingly.

The objectives of the present work are twofold. First of all to establish the quality of initial gas distribution as delivered by common liquid collecting devices. Secondly, to observe the depth of gas maldistribution penetration depending on the type of initial (mal)distribution, and finally to investigate the relation between bed pressure drop and the initial gas maldistribution. In this paper the emphasis is on experimental evidence. A detailed elaboration of CFD modelling related aspects is given in another paper [22].

## EXPERIMENTAL

### Experimental Set-up and Procedure

The necessary experiments were performed using the larger one of two column hydraulics' simulators available at Delft University of Technology. Figure 1 shows a 3-D drawing of this installation. The heart of the experimental set-up is a 1.4 m ID column consisting of a number of flanged Plexiglas sections which allows installation of beds with heights up to 6 m. The transparent part of the column is supported by stainless steel column sump, which is made broader (1.8 m ID) to accommodate gas inlet distributor. With this multipurpose set-up various hydraulic experiments can be carried out with air/water system, at atmospheric pressure and ambient temperature.

Air was supplied to the column by a powerful blower ( $7-8 \text{ m}^3/\text{s}$ ), and the air flow rate was measured by an Annubar flow meter, i.e. a multiple Pitot-tube device placed 5 m below the inlet of a 7 m tall, 0.6 m ID air intake tube. An element of Montz-pak B1-250 was installed downstream of the blower to straighten the flow leaving the blower, on its way through a 0.6 m ID tube to the distribution section in the middle of the bottom part of the column. A vertical gas riser tube ending with Chinese-hat-like structure was used as gas distributor, because of its simplicity and minimum space requirement. Water from the supply tank was pumped through the pipes containing flow meters (two rotameters and a magnetic flow meter) by a centrifugal pump (110

$\text{m}^3/\text{h}$ ) to the top of the column, at an elevation of approximately 10 m. For the purposes of this study water was distributed over the packing using a large liquid load (20 to  $50 \text{ m}^3/\text{m}^2\text{h}$ ) liquid distributor (Sulzer type VKG) with irrigation density of 100 drip points per  $\text{m}^2$ .

Pressure drop over the bed was measured using a fine pressure drop cell integrated into a state of the art digital device connected in parallel to a common U-manometer filled with water. The packing used in this study was Montz-pak B1-250. This packing is made of unperforated sheet metal with a shallow embossed surface with corrugations inclined at an angle of  $45^\circ$ . Packing element height is approximately 0.2 m, and packing layers are assembled of three packing segments. Each packing layer is rotated by  $90^\circ$  to the previous one, which is a common packed bed configuration. In this study the total height was limited to five layers, i.e. 1 m.

As mentioned before, a liquid collector placed above a liquid distributor acts also as the redistributor for gas phase leaving the liquid redistribution section. In vacuum applications, low-pressure vane-type liquid collectors are preferred, however, traditionally the chimney tray structures are often used in situations where the pressure drop is not critical. Figure 2 shows a 3-D drawing indicating major geometrical features of liquid collectors employed in this study. The accompanying table indicates the percent of free area available for gas flow. One should note that the liquid collector with the  $80^\circ$  inclination angle of blades contains on each side one row of blades more than  $60^\circ$  configuration. The chimney tray collector comprises a number of uniformly positioned elongated gas risers provided with flat covers.

The cross sectional distribution of air velocity was measured under dry conditions with a Pitot-tube moving in regular time intervals over a fine, square pitch measurement grid (spacing 2.4 cm). The measurements were taken at the distance from the collector corresponding roughly with the packing support position (30 - 40 cm, depending on the type of the collector). It should be noted that this implies around 2450 measurement points for one cross section, which was done automatically and took approximately 14 hours per run. Measured local velocities are presented in form of 2-D plots made in Excel, using the color scheme equivalent to that established in presenting the similar CFD data. In this case, the variations in velocity are indicated by different colors covering a range from 0 (dark blue) to highest velocity in bright red. In black-white pictures black areas correspond with no velocity zones. Light areas with different degrees of shading indicate different velocity zones; the darker the shaded area the higher the velocity.

The depth-of-penetration-experiments were carried out under dry conditions by building the bed layer by layer. In each case, the velocity profile leaving the packing was measured directly above the packing (1 cm distance). In addition to a "normal" profile, as delivered by the  $80^\circ$  vane-type collector, three characteristic large-scale maldistribution profiles were introduced by placing thin metal plate with desired pattern of free area below the first layer of packing. These three "maldistribution generators" all reducing the available cross sectional area by 50% and introducing approximately the same amount of form drag are shown in Fig. 3, together with corresponding gas distribution profiles. Shaded areas are closed for gas flow. The depicted profiles represent velocities measured immediately above the maldistribution generation plates placed on the packing support structure. Due to a

factor 2 larger cross sectional area the range of employed velocities is much lower in normal case. Obviously, only in case of 24 symmetrically distributed holes, with a diameter of 20 cm, the velocity profile entering the bed may be considered as a representative of uniformly distributed large-scale maldistribution, with certain degree of small-scale maldistribution in nearly each hole. Other three including the normal situation are examples of a tremendously maldistributed velocity profile. The center blockage profile resembles to some extent that kidney-like obtained under normal condition, however with all of the gas flow entering the bed via the periphery at a more than factor 2 larger average velocity. Certainly the worst case is the profile obtained by so called chordal blockage, i.e. by closing one half of the cross sectional area. In this case the whole gas flow enters on one side of the bed only.

### Gas Maldistribution Characterization

2-D plots as those used in Fig. 3, particularly colored ones, are useful means to visualize the cross sectional distribution of velocity. Common one-dimensional way to quantify the maldistribution is to make use of the well-known maldistribution factor, i.e. the coefficient of variation of the velocity measurements. For a column cross section with a grid superimposed the coefficient of variation,  $C_v$ , is defined as

$$C_v = \left[ \frac{1}{A_t} \sum_{i=1}^N A_i \left( \frac{u_i - \bar{u}}{\bar{u}} \right)^2 \right]^{0.5} \quad (1)$$

where  $A_t$  is the total cross sectional area,  $A_i$  is the area of a cell,  $u_i$  is local, cell velocity, and  $N$  is the total number of cells. The overall mean velocity is defined as

$$\bar{u} = \frac{1}{A_t} \sum_{i=1}^N A_i u_i \quad (2)$$

A  $C_v$  approaching zero indicates a uniform (plug) flow situation. Since  $C_v$ , which is a measure for the magnitude of maldistribution does not give any idea about cross sectional distribution of flow variations, i.e. the nature of the maldistribution, Billingham et al [3] introduced a new coefficient  $C_m$  that distinguishes between small- and large-scale forms of maldistribution.  $C_m$  is evaluated in an identical manner as the coefficient of variation,  $C_v$ , except a local mean velocity rather than an overall mean velocity is used in its calculation. The corresponding expression is

$$C_m = \left[ \frac{1}{A_t} \sum_{i=1}^N A_i \left( \frac{u_i - \bar{u}_i}{\bar{u}_i} \right)^2 \right]^{0.5} \quad (3)$$

where  $\bar{u}_i$  is the local mean velocity associated with cell  $i$ , calculated by

$$\bar{u}_i = \frac{\sum \delta_{ij} (A_i u_i + A_j u_j)}{\sum \delta_{ij} (A_i + A_j)} \quad (4)$$

where  $\delta_{ij} = 1$ , if  $i$  and  $j$  are neighbours, and  $\delta_{ij} = 0$ , if  $i$  equals  $j$  or the cells do not share a common border. Namely, regarding the contribution of neighbouring cells,

distinction is made between three characteristic situations. Corresponding contributions are described by the following expressions, as defined for cells M, T and E according to the accompanying grid:

A	B	C	D	E
F	G	H	I	J
K	L	<b>M</b>	N	O
P	Q	R	S	<b>T</b>
U	V	W	X	Y

$$\begin{aligned}
 \bar{u}_M &= \frac{(u_M + u_H) + (u_M + u_N) + (u_M + u_R) + (u_M + u_L)}{8} \\
 \bar{u}_T &= \frac{(u_T + u_S) + (u_T + u_O) + (u_M + u_Y)}{6} \\
 \bar{u}_E &= \frac{(u_E + u_D) + (u_E + u_J)}{4}
 \end{aligned} \tag{5}$$

The ratio of  $C_v$  and  $C_m$  is defined as the maldistribution index:

$$MI = \frac{C_v}{C_m} \tag{6}$$

As a ratio of the numbers of the same order of magnitude,  $MI$  reduces the range of absolute values, and the values close to unity represent uniform distribution of flow deviations. In essence, Billingham et al. [3] approach allows for the effect of clustering the flow variations. If the flow variations are clustered into large groups  $C_m$  is much less than  $C_v$ , and this leads to a large  $MI$ , i.e. to a maldistribution more detrimental to column efficiency. The maldistribution index  $MI$  is independent of the magnitude of the flow variations and is solely a measure of the spatial distribution of these variations. In general, the quality of flow distribution improves with both decreasing  $C_v$  and  $MI$ , however it is difficult to provide general recommendations for initial distribution quality in terms of certain minimum values of these two in a way interrelated parameters. The results reported by Fan et al [10] indicate  $C_v$  values going from 200% for different gas-sparger devices down to 37% for a quite sophisticated circular device. Interestingly, the latter one was achieved in conjunction with a rather low pressure drop.

## RESULTS AND DISCUSSION

### Gas Distribution Performance of Liquid Collectors

Gas distribution performance of three liquid collectors is shown in Figure 4 in form of 2-D velocity plots, representing normalised velocities at a distance from the collector corresponding to the location of packing support. To obtain the local velocities the numbers from the legend should be multiplied by the given value of the superficial gas velocity (2.5 m/s). As shown in Figure 4, vane-type collectors create a kidney-like profile, with high velocity zones mainly at periphery, while for the chimney tray the high velocity region is concentrated around the centre. Corresponding maldistribution factor and maldistribution index values are shown in Table 1, indicating roughly the same extent of maldistribution in all three cases. Obviously, all three devices produce an immense large-scale maldistribution.

Pronounced difference in  $C_v$  values of two vane-type collectors correlates with the difference in velocities observed at the periphery, which indicates the effect of the

vane inclination angle. Namely, the 60° configuration directs a relatively larger part of air stream toward the column walls than the 80° vanes.

Anyhow, the degree of maldistribution associated with chimney tray collector is surprisingly large regarding the extent of associated pressure drop. As indicated in Figure 5, the dry pressure drop of the chimney tray collector is roughly 50 % larger than that of vane-type collectors. So it appears that pressure drop of the distribution device itself is not a direct measure for the quality of gas distribution, as generally believed. As demonstrated in another paper [22], the degree of reduction of cross sectional area in conjunction with gas risers design and layout plays also an important role. However, it should be noted that the layout of the chimney tray collector considered here is not the optimal one. Namely, it was designed to fit into existing redistribution section configuration designed originally for vane type liquid collectors. However, the open area of 25 % is in accordance with common design practices.

Unfortunately, it was not possible to measure the gas distribution pattern under a dry or even better an irrigated bed. In absence of any downstream pressure drop the measured profiles represent actually the worst case. However, a study by Suess [9] indicated a very high liquid load is required to affect the inlet gas distribution profile significantly.

Dry experiments were carried out to get an idea about the extent of the smoothing out effect of a packing layer with respect to the form of severe initial maldistribution as imposed by vane-type and chimney tray liquid collectors. Figure 6 shows 2-D images of velocity distribution after one layer of packing, measured 1 cm above the packing, with corrugated sheets placed in parallel with the orientation of gas risers, and rotated by respectively 45 and 90 degrees with respect to the orientation of gas risers. Table 2 shows the corresponding values of maldistribution factor and maldistribution index. For comparison, the corresponding values for 80° vane-type collectors are added. Obviously, in both cases there is a profound smoothing out effect of one packing layer, which is however most pronounced in case of the packing rotated by 45°. This case clearly illustrates the nature and the added value of the maldistribution index,  $MI$ , as a means for characterisation of maldistribution. Here, in terms of changes in absolute values of inlet maldistribution factor ( $C_v$ ) and maldistribution index ( $MI$ ), the overall improvement is more pronounced in case of the 80° vane-type collector. The numbers in the parentheses in Table 2 indicate roughly the same level of improvement in the profile generated by the 60° vane-type collector. It should be noted that within the range investigated (F-factor = 1.5 – 3.8 Pa<sup>0.5</sup>) both  $C_v$  and  $MI$  appeared to be practically insensitive to changes in gas load.

Regarding the degree of disintegration and dispersion of high velocity clusters and resulting evenness in distribution of low and high velocity zones, the first layer rotation by 45° appears to be the best solution. Hence, a 45° rotation of the first layer of packing is recommend as general practice for installation of structured packings. This practice was exercised throughout this study. From the same reason, the liquid distributor was placed above the packing so that the troughs were rotated by 45° with respect to the orientation of corrugated sheets in the first layer of packing on the top of the bed.

### **Relation between the Initial Maldistribution and Pressure Drop**

An indication of the effect of the type of initial maldistribution on column hydraulics' can be obtained from the Figure 7, which shows the pressure drop of a 1 m bed placed above the liquid collectors considered in this study. Dry pressure drop is some 10 % lower in case of initial maldistribution as generated by the chimney tray, however this changes into opposite situation under wet conditions and becomes slightly more pronounced at very high liquid load. In all cases the loading point, i.e. the capacity was not affected by the type of initial maldistribution.

Obviously, the difference between dry and wet pressure drop at the same gas load is much larger in case of the initial profile as delivered by chimney tray, where the bulk of gas is entering through the central zone of the packing. This indicates a stronger interaction of entering gas and leaving liquid streams. The gas flow concentrated in the central part forces the liquid to concentrate on periphery, at least in the bottom layer. Similar behaviour but opposite effect was observed with vane type collectors. Namely, visual observations indicated clearly that gas flow entering the packing at the periphery forces the liquid to drain mainly through the central zone of the first packing layer from below.

However it is difficult to say whether the liquid deflecting effect is limited to first packing layer only. A relatively larger, irrigated-bed pressure drop in case of chimney tray collector suggests that this could be the case. Namely, the liquid concentrated in the annulus surrounding the central zone could lead to a limitation in the further lateral spreading of gas. With a strong main stream of gas flowing upwardly confined in the central zone a relatively larger mean velocity is maintained resulting in a higher velocity head and consequently a correspondingly larger pressure drop. So it may be that in high gas velocity situations the liquid distribution pattern in bottom layers is significantly influenced by a strongly maldistributed inlet gas flow.

### **Controlled Gas Maldistribution Study**

Results of controlled gas maldistribution studies are shown in Figures 8 and 9 in form of 2-D velocity plots, per packing layer. Due to the total height limitation, the bed height was limited to five packing layers. Figure 8 indicates the depth of penetration of initial maldistribution for normal situation and the multi-hole maldistribution generator, and the same is given in Fig. 9 for an annular (centre blockage) and a half-circled (chordal blockage) initial gas profile. The corresponding rounded  $C_v$ ,  $C_m$ , and  $MI$  values are shown in Table 3. It should be noted that here the "normal situation" refers to the 80° vane-type collector used in conjunction with maldistribution generators employed. Also the values for zero and the first layer are somewhat larger than those shown in Tables 1 and 2, respectively, for 80° vane-type collector. This is the consequence of some mechanical provisions made in the meantime in the redistribution section to enable easier installation/exchange of collectors.

As shown in Fig. 8, the kidney-like initial profile produced by the 80° vane collector is smoothed out after two packing layers. The same occurs with uniformly distributed large-scale maldistribution introduced by the multi-hole maldistribution generation plate. As illustrated in Fig. 9, the consequences of a centre blockage are visible after three packing layers, while the chordal blockage introduced an inclined velocity profile visible after 5 packing layers. In the latter case the difference in average velocity between lower and upper end of the profile is still factor 2, which is a very



large difference, certainly an order of magnitude larger than that which could be considered tolerable in case of liquid distribution.

Actually, in all cases one or two more layers would be needed to smooth out the initial maldistribution completely, i.e. to bring it to a level corresponding with the natural (small scale) one for the packing type and size in question. So the  $C_v$  and  $MI$  numbers shown in Table 3 indicate roughly the values close enough to final ones for B1-250 packing. As expected  $C_v$  values decrease progressively with decreasing range of deviations in local velocities. The behaviour of  $MI$  is not so obvious. Interestingly the highest uniformity of large-scale maldistribution, indicated by a large  $C_m$  value is obtained with multi-hole distributor. In two other cases, with axially symmetrical form of large-scale maldistribution, however of a much larger extent (normal and annular), the  $C_m$  increases with bed height, but with a less pronounced decrease in  $C_v$  values this leads to fast approach of a minimum value of  $MI$ . In case of an unsymmetrical inlet profile, as created by chordal blockage, there is a steady, but less pronounced decrease in  $C_v$  value, while the value of  $C_m$  remains more or less unchanged. This indicates certain degree of persistence in form of large-scale spatial maldistribution clearly visible in 2-D plots shown on the left-hand side in Fig. 9.

An indication of the magnitude of pressure drop associated with the extent of maldistribution observed per packing layer in conjunction with imposed initial maldistribution profiles is shown in Fig. 10, for a constant gas load. For normal situation, the pressure drop per layer is practically constant and at lowest level of all. Practically the same level of pressure drop is achieved after second packing layer in case of highly symmetrical inlet profile created by multi-hole maldistribution generator. This is not surprising if we consider the fact that the gas entering the second layer is spread over the whole cross section of the column. The annular inlet profile imposed by centre blockage needs a layer more to cover the whole cross section. For the chordal blockage this process is completed within four packing layers, however additional effort, i.e. bed height is needed to equalise the remaining difference in mean velocities in two halves of the column cross section. The amount of pressure drop involved in this case is in some proportion with the extent of lateral transport, i.e. distance involved. This is nearly factor 3 larger than that involved in case of a annular type of inlet profile, with the of similar degree of large scale maldistribution, but axially symmetrical in form.

Certainly, the pressure drop profiles shown in Fig. 10 correspond in trend with observed degree of improvement in uniformity of gas flow. There is a clear correlation between the magnitude of maldistribution and the pressure drop. An inspection of  $C_v$ ,  $MI$  and pressure drop values associated with profiles leaving second layer of packing suggests existence of some relation between the magnitude of pressure drop and the degree of severity in spatial maldistribution. However, the available data do not provide a sufficient basis for establishing a quantitative relation between the pressure drop and the magnitude of either  $C_v$  or  $MI$ . This fact indicates shortcomings of both means for maldistribution characterisation and pleads for additional effort toward establishing a more suitable maldistribution characterisation means, which should combine appropriately both aspects, i.e. the magnitude and the extent of large-scale maldistribution into a single measure of the degree of severity of maldistribution.

Figure 11 shows the dry pressure drop of the 1 m bed as a function of the gas load with the type of initial gas profile as a parameter. It should be noted that the curves represent the pressure drop of the bed only, obtained by subtracting the pressure drop generated by respective maldistribution generator from the total pressure drop. As already indicated, the overall pressure drop increases with the degree of severity of gas maldistribution in the bed. As shown in Figures 12, the irrigated bed pressure drop corresponding to a liquid load of  $20 \text{ m}^3/\text{m}^2\text{h}$ , follows the same trend. However, as it can be seen by comparing the wet and dry pressure drop curves for a constant value of gas load in the preloading region, say F-factor = 1, the difference between wet and dry pressure drop is more pronounced for centre and chordal blockage cases. In general, due to abrupt reduction in available cross sectional area and associated liquid drainage problems the onset of loading occurs at much lower gas load than normally. Added curve for the chordal blockage case indicates the degree of premature loading in case of an extremely high liquid load ( $50 \text{ m}^3/\text{m}^2\text{h}$ ).

An interesting aspect of the FRI study [20] mentioned before is that the capacity remained unaffected by a 30% chordal blockage of the column cross section between gas inlet and packing. This is not surprising if we consider the fact the construction applied at FRI allowed the liquid to drain undisturbed from gas in the segment of cross section blocked for gas flow.

## CONCLUSIONS

Common low- and high pressure drop liquid collectors generate gas maldistribution of strikingly large extent, which is an order of magnitude or even larger than that associated with liquid distribution standards.

Due to a high degree of axial symmetry the heavily maldistributed inlet gas profiles are smoothed out within two packing layers. The best effect is achieved with the first layer rotated by 45 degrees relative to the orientation of vanes or chimneys.

A chordal blockage of 50% of cross section area generates a maldistribution that penetrates deep into the bed consisting of structured packing.

Both dry and wet pressure drop of a structured packing bed increase with the degree of severity of initial gas distribution.

Large size random packings and structured packings with a very open surface area may be more sensitive to initial gas maldistribution than the B1-250 with its unperforated surface, which ensures maximal lateral transport of gas within one packing layer.

The coefficient of flow variation (maldistribution factor)  $C_v$  in combination with the maldistribution index  $MI$  gives a good indication of the quality of gas distribution.

## ACKNOWLEDGMENT

The authors would like to thank BASF, BAYER, DSM, DEGUSSA, KOCH-GLITSCH, MONTZ, PRAXAIR, SG NORPRO, SHELL, and SULZER for supporting this work. The equipment used in this study was donated by J. Montz (packing, liquid distributor and vane-type collectors), Koch-Glitsch (chimney tray collector), and Sulzer Chemtech (high liquid load distributor).

## NOMENCLATURE

$A_i$	cell area, m <sup>2</sup>
$A_t$	total column cross sectional area, m <sup>2</sup>
$C_v$	coefficient of variation, -
$C_m$	coefficient of maldistribution, -
$F$ -factor	( $=u_{Gs} \rho_G^{0.5}$ ) gas load factor, (m/s)(kg/m <sup>3</sup> ) <sup>0.5</sup> or Pa <sup>0.5</sup>
$Ml$	maldistribution index, -
$N$	total number of cells, -
$u$	mean velocity, m/s
$u_{Gs}$	superficial gas velocity, m/s
$u_i$	local mean (cell) velocity, m/s
$\delta_{ij}$	operator in Eq. (4)

## REFERENCES

1. Z. Olujic, J. de Graauw (1990), "Experimental Studies on the Interaction Between the Initial Liquid Distribution and the Performance of Structured Packing", Separation Science and Technology 25, 1723-1735.
2. C. W. Fitz, D. W. King, and J. G. Kunesh (1999), "Controlled Liquid Maldistribution Studies on Structured Packing", Trans. ICHME 77 (Part A) 482-486.
3. J. F. Billingham, D. P. Bonaquist, and M. J. Lockett (2001), "Characterization of the Performance of Packed Distillation Column Liquid Distributors", ICHME Symposium Series No. 128, B841-851.
4. D. P. Edwards, K. R. Krishnamurthy, and R. W. Potthoff (1999), "Development of an Improved Method to Quantify Maldistribution and its Effect on Structured Packing Performance", Transactions of ICHME/Chem. Eng. Res. Des. 77 (Part A) 656-662.
5. J. F. Billingham and M. J. Lockett (2001), "A Simple Method to Assess the Sensitivity of Packed Distillation Columns to Maldistribution", Presented at AIChE Annual Meeting, Reno (Nevada) November 4-9, Paper No. 18a.
6. A. Muir and C. L. Briens (1986), "Low Pressure Drop Gas Distributors for Packed Distillation Columns", The Canadian J. Chem. Eng. 64, 1027-1032.
7. F. Moore and F. Rukovena, F. (1987), "Liquid and Gas Distribution in Commercial Packed Towers", Chemical Plants & Processing, August 11-15.
8. K. E. Porter, Q. H. Ali, A. O. Hassan and A. F. Aryan (1993), "Gas Distribution in Shallow Packed Beds", Ind. Eng. Chem. Res. 32, 2408-2417.

9. Ph. Suess (1992), "Analysis of Gas Entries of Packed Columns for Two Phase Flow", ICHME Symposium Series No. 128, A369-383.
10. L. Fan, G. Chen, S. Constanzo, and A. Lee (1997), "Hydraulic performance of Gas Feed Distribution Devices", ICHME Symposium Series No. 142, 899-910.
11. X. Yuan and W. Li (1997), "The Influence of Various Gas Inlets on Gas Distribution in Packed Columns", ICHME Symposium Series No. 142, 931-938.
12. R. Darakchiev and C. Dodev (2002), "Gas Flow Distribution in Packed Columns", Chem. Eng. Processing 41, 385-393.
13. R. M. Stikkelman, J. de Graauw, Z. Olujic, H. Teeuw and J. A. Wesselingh (1989), A study of Gas and Liquid Distribution in Structured Packing, Chem. Eng. Technol. 12, 445-449.
14. Z. Olujic, F. Stoter and J. de Graauw (1991), "Gas Distribution in Large-Diameter Packed Columns", GAS Separation & Purification 5, 58-66.
15. F. Stoter, Z. Olujic and J. de Graauw (1992), "Modelling of Hydraulic and Separation Performance of Large Diameter Columns Containing Structured Packings", ICHME Symposium Series No. 128, A201-210.
16. Z. Olujic, F. Stoter and J. de Graauw (1992), "Measurement of Large Scale Gas and Liquid Maldistribution in Structured Packings", ICHME Symposium Series No. 128, B151-158.
17. F. Stoter, Z. Olujic and J. de Graauw (1993), "Modelling and Measurement of Gas Flow Distribution in Corrugated Sheet Structured Packings", The Chem. Eng. Journal 53, 55-66.
18. F. J. Zuiderweg, J. G. Kunesh, and D. W. King (1993), "Model for the Calculation of the Effect Maldistribution on the Efficiency of a Packed Column", Trans. ICHME 71 (part A) 38-44.
19. T. J. Cai, C. W. Fitz and J. G. Kunesh (2001), "Vapor Maldistribution Studies on Structured and Random Packings", Proceedings of the Separations Technology Topical Conference, AIChE Annual Meeting, Reno (Nevada), November 4-9, pp. 51-56.
20. A. Mohamed Ali, P. J. Jansens and Z. Olujic (2001), "The Use of Computational Fluid Dynamics to Model Gas Flow Distribution in Packed Columns", Proceedings (CD ROM) of the 6<sup>th</sup> World Congress of Chemical Engineering, 23-28 September 2001, Melbourne, Australia.
21. Z. Olujic, A. Mohamed Ali and P. J. Jansens (2002), "CFD simulation software - A Design Tool for Packed Column Internals?", Proceedings of the Topical Conference "Distillation Tools for Practicing Engineer", AIChE Spring National Meeting, New Orleans, March 10-14, pp.
22. A. Mohamed Ali, P. J. Jansens and Z. Olujic (2002), "Experimental Characterisation and CFD modelling of Gas Distribution Performance of Liquid Distributors and Collectors in Packed Columns", Proceedings (CD ROM) of the 6<sup>th</sup> Distillation and Absorption Conference, Baden-Baden, Germany, 30 September to 2 October, 2000, pp. (*this conference !*)

*Table 1 Extent of gas maldistribution generated by the three liquid collectors used in this study: vane-type (LC-60° and LC-80°) with different blade inclination angles and the chimney tray type (LC-CT)*

	<b>LC-60°</b>	<b>LC-80°</b>	<b>LC-CT</b>
<b>C<sub>v</sub></b>	95	79	80
<b>C<sub>m</sub></b>	12.4	10	12.3
<b>MI</b>	7.6	7.8	6.5

*Table 2 Effect of the angle of rotation of the first packing layer on the extent of gas maldistribution introduced by the liquid collectors studied*

Angle	0°		45°		90°	
Type	<b>LC-80</b>	<b>LC-CT</b>	<b>LC-80 (60)</b>	<b>LC-CT</b>	<b>LC-80</b>	<b>LC-CT</b>
<b>C<sub>v</sub></b>	29	39	29 (35)	32	32	30
<b>C<sub>m</sub></b>	17	24	24 (27)	25	19	16
<b>MI</b>	1.7	1.6	1.2 (1.3)	1.3	1.7	1.9

*Table 3 Extent of gas maldistribution penetration into a bed associated with various forms of initial large scale maldistribution*

<b>Layer/Inlet device</b>	<b>Normal</b>	<b>Multi-hole</b>	<b>Annular</b>	<b>Half-circle</b>
	<i>C<sub>v</sub> / C<sub>m</sub> / MI</i>	<i>C<sub>v</sub> / C<sub>m</sub> / MI</i>	<i>C<sub>v</sub> / C<sub>m</sub> / MI</i>	<i>C<sub>v</sub> / C<sub>m</sub> / MI</i>
<b>0</b>	88 / 16 / 5.6	99 / 40 / 2.5	110 / 17 / 6.5	128 / 19 / 6.7
<b>1</b>	39 / 28 / 1.4	49 / 33 / 1.5	64 / 17 / 3.8	82 / 23 / 3.6
<b>2</b>	38 / 30 / 1.3	35 / 25 / 1.4	38 / 21 / 1.8	68 / 18 / 3.8
<b>3</b>	-	-	34 / 24 / 1.4	53 / 20 / 2.6
<b>4</b>	-	-	32 / 25 / 1.3	44 / 16 / 2.7
<b>5</b>			-	24 / 8 / 3.0

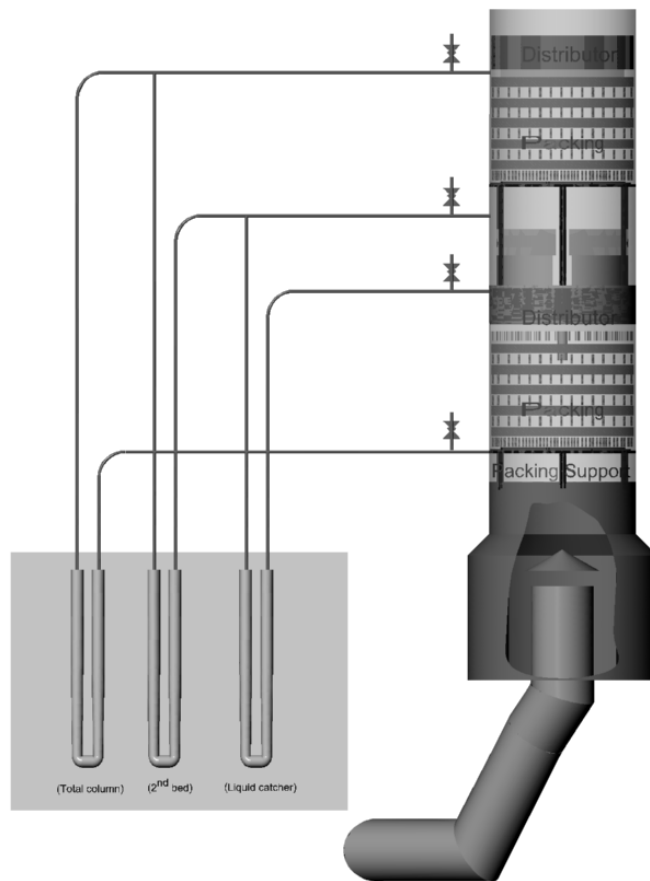
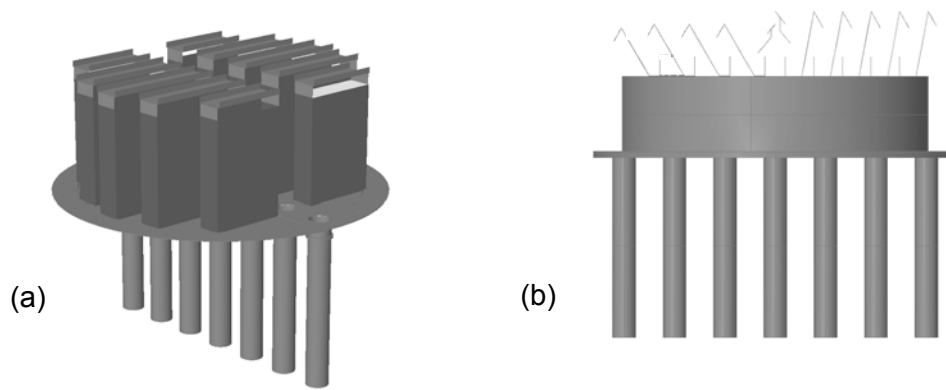


Figure 1: A 3-D impression of the large scale, column hydraulics' simulator configuration used in this study



Open area (%)		
L.C. 60 <sup>o</sup>	L.C. 80 <sup>o</sup>	C.T.
42	26	25

Figure 2: A 3-D impression of the liquid collectors used in this study: (a) a chimney tray (CT), and (b) a vane-type (LC) with respectively 60 and 80 degrees blade inclination

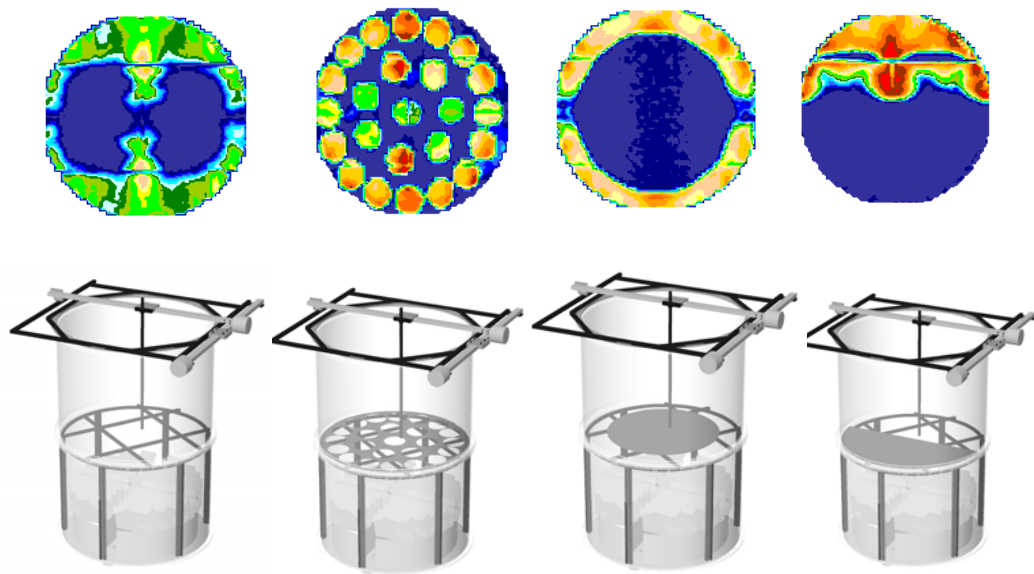


Figure 3: A 3-D impression of the initial maldistribution generation devices used in this study, and corresponding gas velocity profiles

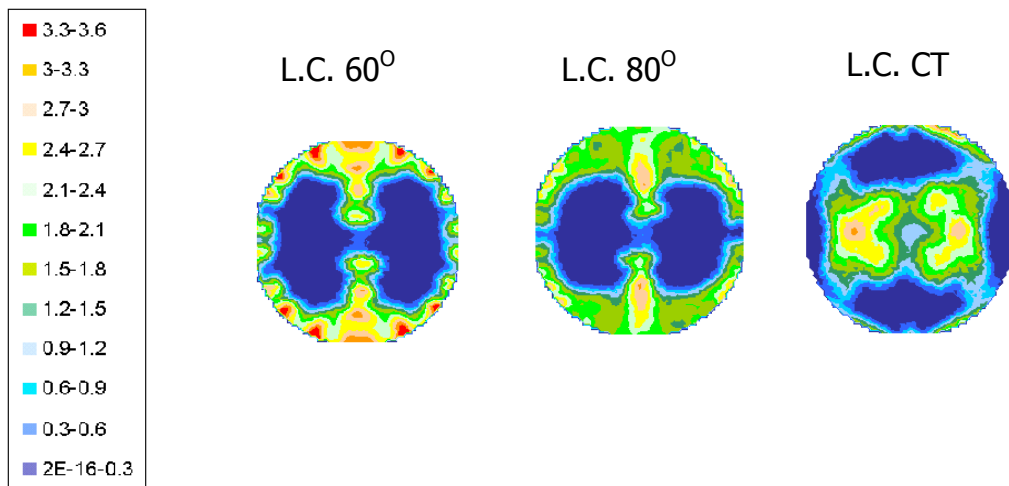


Figure 4: 2-D plots of gas distribution profiles created by liquid collectors used in this study, at a distance corresponding to the position of packed bed support ( $F\text{-factor} = 2.7 \text{ Pa}^{0.5}$ ,  $u_{GS} = 2.5 \text{ m/s}$ )

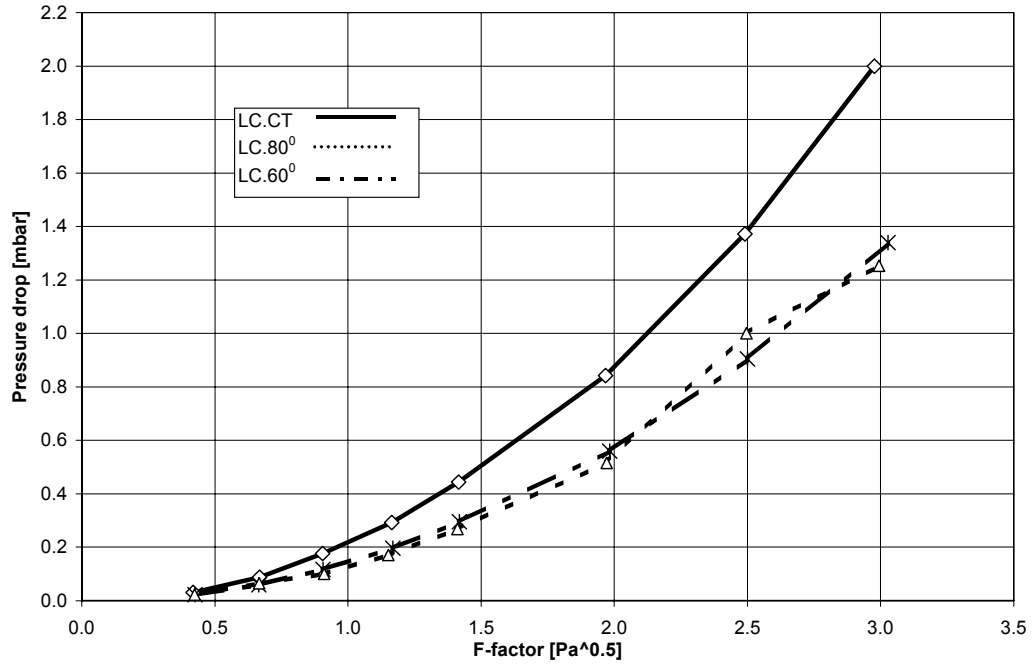


Figure 5: Dry pressure drop of liquid collectors considered in this study

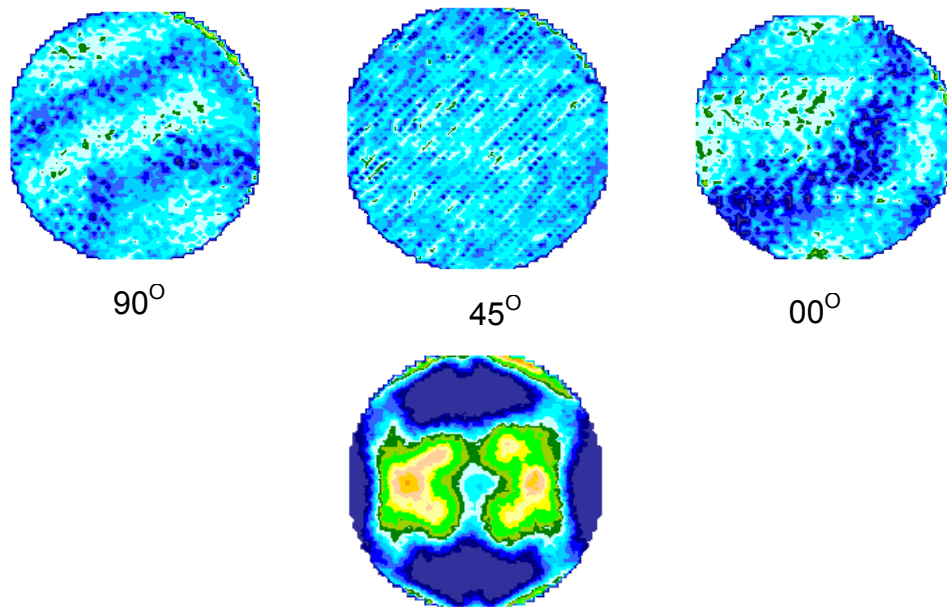


Figure 6: 2-D plots of gas distribution profiles leaving the first layer of packing, for different angles of rotation of packing with respect to chimneys orientation ( $F\text{-factor} = 2.7 \text{ Pa}^{0.5}$ )



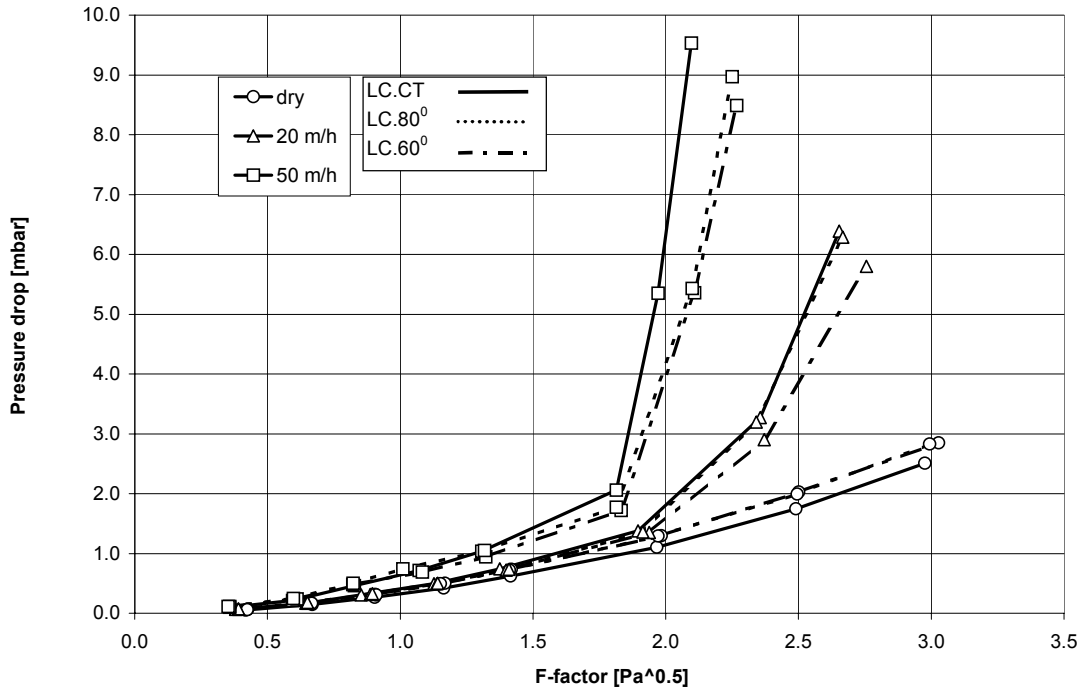


Figure 7: Pressure drop of a 1 m bed placed above the liquid collector as a function of gas and liquid loads for three different initial gas profiles

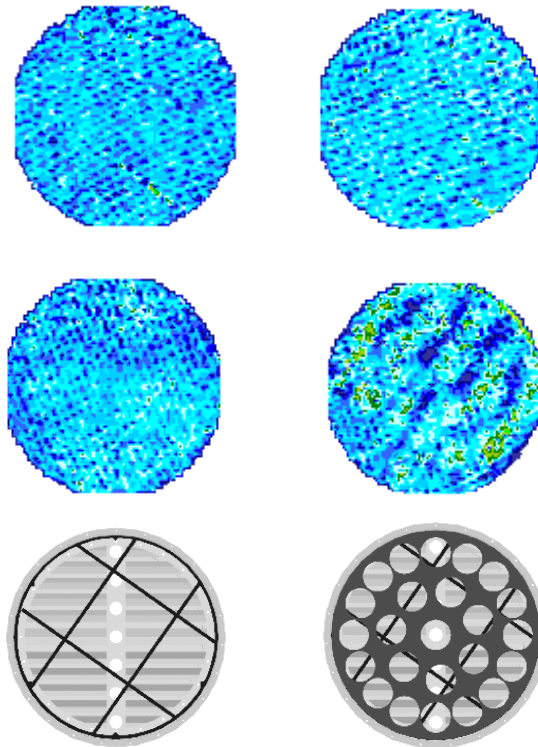


Figure 8: 2-D plots illustrating the depth of penetration of initial maldistribution delivered by the 80° vane-type collector and the multi-hole initial maldistribution generator.

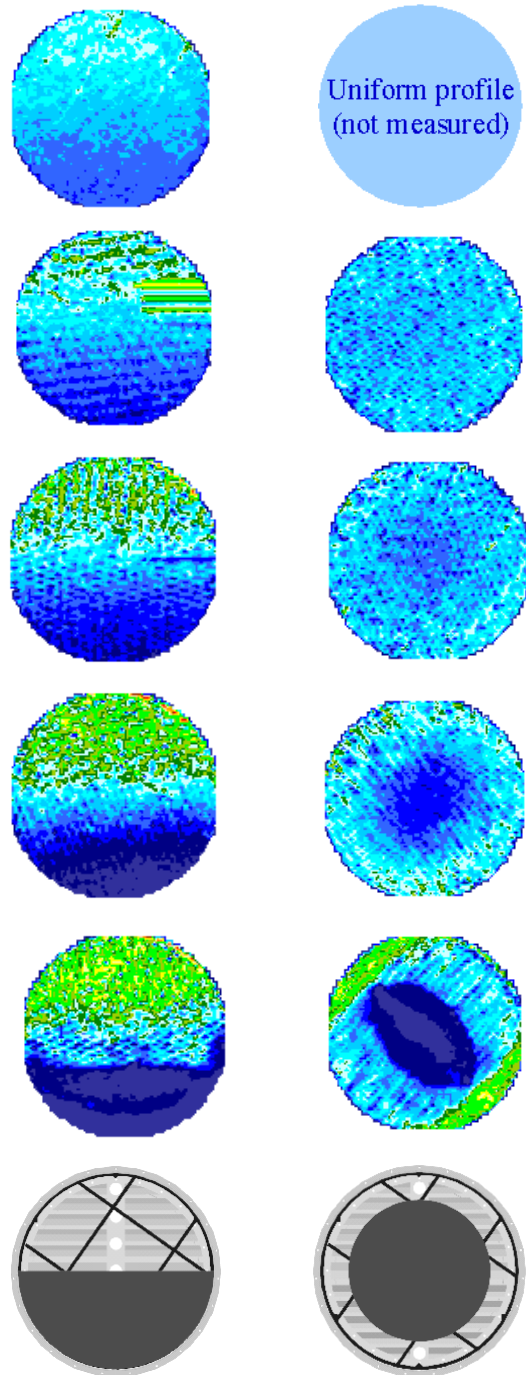


Figure 9: 2-D plots illustrating the depth of penetration of initial maldistribution generated by the centre- and chordal blockage devices.

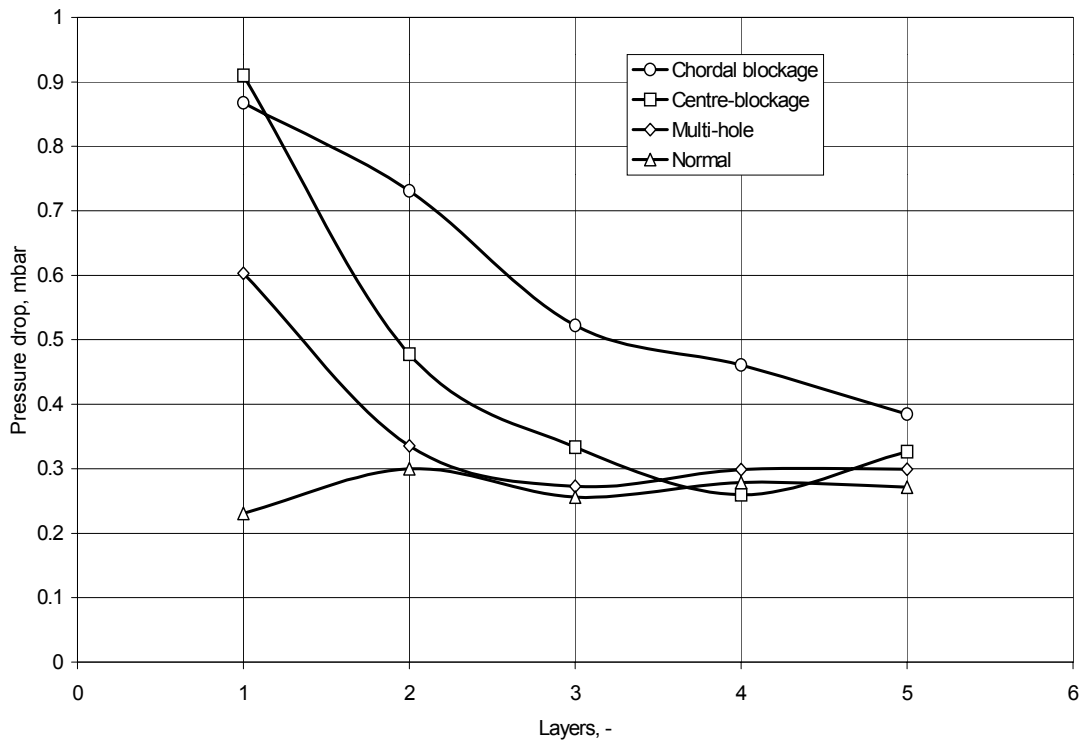


Figure 10: Pressure drop per packing layer for different forms of initial gas maldistribution ( $F$ -factor  $\approx 2 \text{ Pa}^{0.5}$ ).

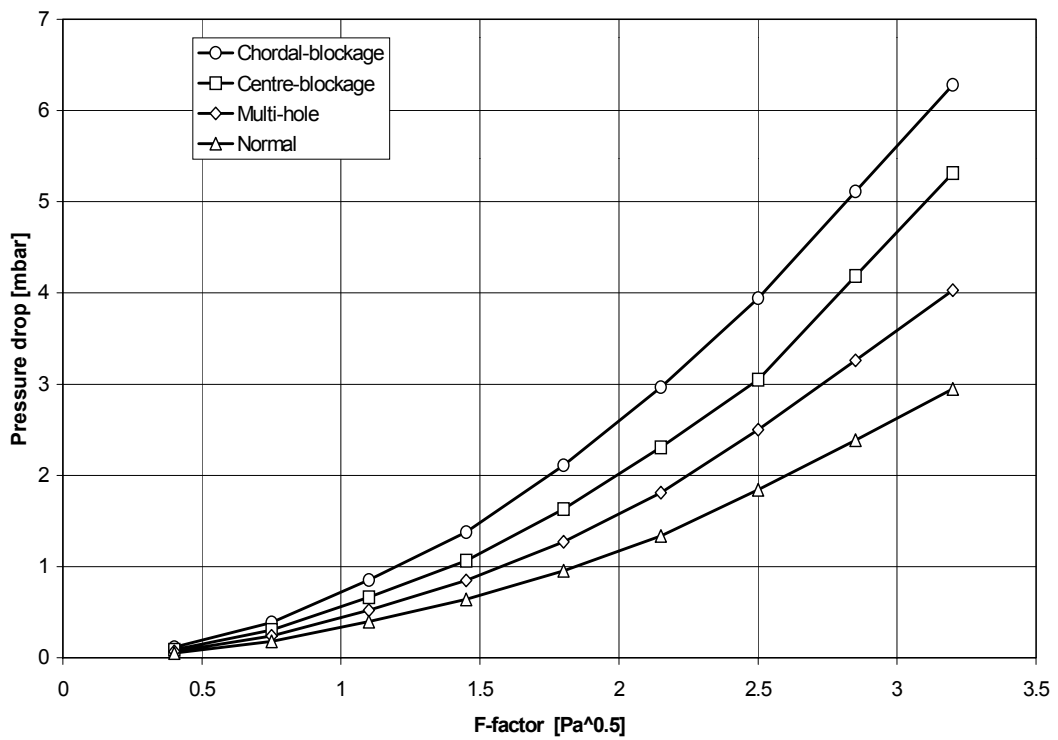


Figure 11: Effect of the form of initial maldistribution on the dry pressure drop of a 1 m bed

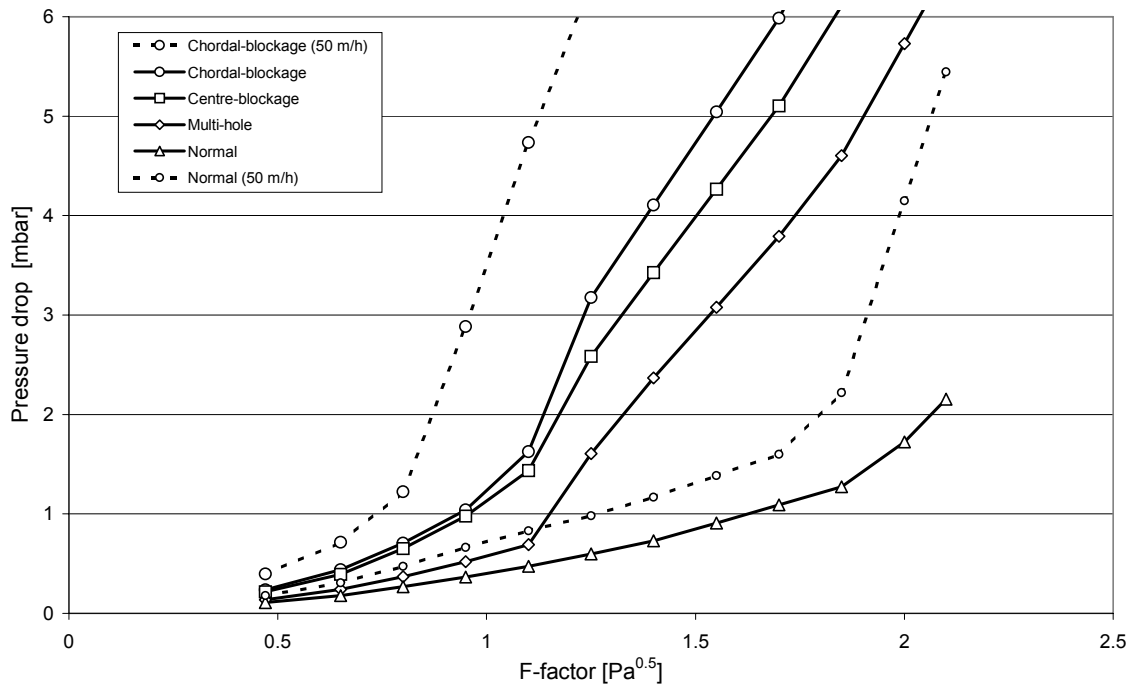


Figure 12: Effect of the form of initial maldistribution on the wet pressure drop of a 1 m bed; the liquid load is 20 m<sup>3</sup>/m<sup>2</sup>h (m/h)